Ice-Binding Surface of Fish Type III Antifreeze

Guangju Chen* and Zongchao Jia#
*Department of Chemistry, Beijing Normal University, Beijing 100875, China, and #Department of Biochemistry, Queen's University, Kingston, Ontario K7L 3N6, Canada

ABSTRACT We employed computational techniques, including molecular docking, energy minimization, and molecular dynamics simulation, to investigate the ice-binding surface of fish type III antifreeze protein (AFP). The putative ice-binding site was previously identified by mutagenesis, structural analysis, and flatness evaluation. Using a high-resolution x-ray structure of fish type III AFP as a model, we calculated the ice-binding interaction energy of 11 surface patches chosen to cover the entire surface of the protein. These various surface patches exhibit small but significantly different ice-binding interaction energies. For both the prism ice plane and an "ice" plane in which water O atoms are randomly positioned, our calculations show that a surface patch containing 14 residues (L19, V20, T18, S42, V41, Q9, P12, A16, M21, T15, Q44, I13, N14, K61) has the most favorable interaction energy and corresponds to the previously identified ice-binding site of type III AFP. Although in general agreement with the earlier studies, our results also suggest that the ice-binding site may be larger than the previously identified "core" cluster that includes mostly hydrophilic residues. The enlargement mainly results from the inclusion of peripheral hydrophobic residues and K61.

INTRODUCTION

Nonequilibrium antifreeze proteins (AFPs) have been found in many organisms. These proteins are able to depress the freezing point of aqueous solutions by inhibiting the growth of existing ice crystal seeds (for a review, see Davies and Hew, 1990). By adsorbing to the ice surface, AFPs are thought to disrupt ice growth by introducing curvatures to the ice surface (Raymond and DeVries, 1977), where ice growth becomes energetically unfavorable and further ice growth is hindered. Whereas other cryoprotectants such as glycerol decrease the freezing point in a colligative manner, AFPs lower the freezing point of a solution without changing the melting point. The difference between the freezing point and the melting point is termed *thermal hysteresis*, which is widely used as an indicator of AFP activity.

Among all AFPs, fish AFPs are the most extensively characterized (Davies and Sykes, 1997), and they can be divided into structurally distinct groups. The first group contains antifreeze glycopeptides and type I AFPs, both of which possess linear helical structures with a periodically repeating ice-binding motif. A second group consisting of globular proteins without any apparent repetitive structural motifs includes type II and type III AFPs. The recently discovered type IV AFP may be considered a chimera between the above two groups, as it is predicted to have an α-helix bundle structure (Deng et al., 1997).

Although AFPs have been studied for more than 20 years, the precise mechanism by which they inhibit ice growth is still unclear. Unlike enzymatic proteins that can often be cocrystallized along with their ligands, there is no direct way to investigate the molecular interactions between AFPs and the growing ice crystals. One approach that was employed over the last several years to bridge this shortcoming is molecular modeling. Simulations such as energy minimization and molecular dynamics have played important roles in characterizing AFP structures and their interactions with ice. These computations have mainly focused on type I AFPs. As the initial x-ray structure (Yang et al., 1998) was of low resolution and lacked side chains, several molecular dynamics studies were performed to establish the equilibrium side-chain positions in both the gaseous state (Chou, 1992; Cheng and Merz, 1997) and the aqueous state (Jorgensen et al., 1993; McDonald et al., 1993; Madura et al., 1996; Cheng and Merz, 1997). These studies proved to be insightful, as they suggest that Thr residues regularly spaced in type I AFPs orient themselves with their side chains protruding from the same side of the α-helix at intervals matching the distance of O atoms on the {20–21} ice plane. Similarly, the energy minimization and molecular dynamics simulations, together with multiple sequence alignments, allowed the creation of a model of the type II AFP based upon their low-sequence homology to the carbohydrate recognition domain of C-type lectins (Sönnichsen et al., 1995). The interaction with ice of type II AFP was investigated by computation (Wierzbicki et al., 1997). Furthermore, the energy minimization and molecular dynamics simulation have also been carried out to establish the stability of type III AFPs in aqueous solutions (Madura et al., 1996).

In addition to the studies of AFP alone in gaseous and in aqueous states, molecular modeling has been extended to investigate AFP-ice interactions. Such studies generally involve the manual positioning of an AFP molecule in close proximity to its suspected docking position on an ice surface, followed by lengthy energy minimization and molecular dynamics simulations. Critical to these studies are the

Received for publication 11 January 1999 and in final form 15 June 1999.
Address reprint requests to Dr. Zongchao Jia, Department of Biochemistry, Queen's University, Kingston, ON K7L 3N6, Canada. Tel.: +1-613-533-6277; Fax: +1-613-533-2497; E-mail: jia@crystal.biochem.queensu.ca.

0006-3495/99/09/1602/07 $2.00

appropriate choices of both the ice-binding site of the AFP in question and the ice plane to which docking takes place. For type I AFPs, it is generally believed that the AFP face containing the polar Thr residues interacts with the {20–21} ice plane to inhibit crystal growth, because of both ice-etching experiments and geometric considerations. Combined with the ice-etching results of type I AFP (Knight et al., 1991), several early docking models of type I AFP were achieved through molecular dynamics computations (e.g., Chou, 1992). Lal et al. (1993) used energy minimization and molecular dynamics simulations to demonstrate the energetic preference of type I AFPs for the {20–21} ice plane over both the basal and prism planes. Several studies (Wen and Laursen, 1992; Madura et al., 1994; Wierzbicki et al., 1996; Cheng and Merz, 1997) investigated the detailed mechanism of type I AFP binding to the {20–21} ice plane and reported that it has an energetic preference for binding in the ⟨01–12⟩ direction, as initially suggested by Knight et al. (1991). All of these studies involving type I AFP emphasized the importance of hydrogen bonding in accounting for the presumed strong protein-ice coupling. Most also noted excellent shape complementarity between the AFPs and ice, implying perhaps a significant role for van der Waals interactions as well.

Although less extensively studied than type I AFPs, type III AFPs have also been investigated with molecular modeling for its interactions with ice. For this AFP, however, the docking procedure is somewhat more complicated. Unlike type I AFP, neither the ice-binding surface nor the ice plane at which binding takes place has been established unequivocally. Ice-etching studies have been inconclusive with regard to the ice plane involved in type III AFP binding (Cheng and DeVries, 1991). Extensive mutagenesis experiments have identified several residues located on one flat amphipathic plane as being important to AFP activity (e.g., Graether et al., 1999), but it was difficult to knock out the antifreeze activity completely through mutation in the putative ice-binding site. These uncertainties aside, Madura et al. (1996) investigated the prism plane binding of type III AFP, using energy minimization and molecular dynamics simulations. Although no specific conclusions could be drawn, emphasis was placed on the need for a favorable orientation that maximizes the hydrogen bond and van der Waals interactions. Sönnichsen et al. (1996) investigated the prism plane binding by this putative ice-binding site and concluded that hydrophobic groups might play a more significant role in protein-ice interactions than previously thought. Furthermore, mainly by geometric considerations, Jia et al. (1996) proposed a model for type III AFP-ice binding that involves five hydrogen-bonding atoms on the putative ice-binding site aligned with two ranks of ice O atoms on the prism plane. In addition, other inventive studies have been performed to further characterize the type III AFP-ice interactions. The use of a neural network to relate the wild-type and mutant characteristics to type III AFP activity found hydrophobicity to be essential for AFP activity (Graether et al., 1999). Through computational analysis Yang et al. (1998) suggested that "flatness" may in fact be the most important AFP characteristic. In general, partly because of its unremarkable surface structure and the lack of any conclusive experimental evidence, type III AFP interactions with ice remain largely a mystery.

Our present study attempts to approach the question of type III AFP binding from a different perspective. All previous modeling experiments have taken into consideration the putative ice-binding site as a given fact; consequently, no other surface of the AFP has been explored through modeling. Our intention is to determine, without any bias, the best or most energetically favorable ice-binding surface of type III AFP. Therefore, no prior knowledge of known ice-binding residues has been taken into consideration. It was hoped that this systematic approach will be able to shed some definitive light on this enigmatic problem.

COMPUTATIONAL DETAILS

Choice of ice

The primary prism ice plane was constructed from the fractional coordinates of ice using Sybyl, version 6.4 (Tripos, St. Louis, MO). The space group used for ice, I_h, is $P6_{3/mmc}$, with unit cell dimensions $a = b = 4.516$ Å, $c = 7.345$ Å, $\alpha = \beta = 90°$, $\gamma = 120°$. The fractional coordinates used were O (0.3333, 0.6667, 0.0629), H_a (0.3333, 0.6667, 0.1989), and H_b (0.4551, 0.9102, 0.0182). An ice slab with approximate dimensions of $34.0 \times 35.0 \times 7.8$ Å^3 was constructed, containing 480 water molecules, which was large enough to accommodate the largest surface of the AFP. This ice slab is termed "prism" ice.

The second ice slab is termed "random" ice, in which water molecules are randomly positioned. However, the density of the random ice slab was approximately equivalent to that of prism ice ($P6_{3/mm}$). Such a random ice slab was also made using Sybyl, version 6.4 (Tripos), which included 333 water molecules with approximate dimensions of $32.0 \times 32.0 \times 6.2$ Å^3, larger than any surface patch of the AFP.

AFP structure

The structure of fish type III AFP, a small protein consisting of 66 residues, has been determined by both x-ray crystallography (Jia et al., 1996; Yang et al., 1998) and NMR (Sönnichsen et al., 1996). The model of type III AFP used in this study was the 1.25-Å-resolution x-ray structure (Jia et al., 1996).

Choice of AFP surface sites and their docking to ice

Our intention was to systematically study surface sites of the AFP, regardless of whether they have been implicated in ice binding or not. We selected 11 surface patches centered on 11 surface-exposed AFP residues, as indicated in Table

1. These residues are spaced throughout the surface of the AFP to ensure a complete surface coverage of the AFP. Using the protein surface analysis program Grasp (Nicholls et al., 1993), it was evident that these surface patches overlap, and together they cover the entire AFP surface. This was not surprising, as type III AFP is a very small protein. As expected, many residues are included in various patches more than once (Table 1).

All surface patches were manually brought to the vicinity of either a prism ice plane or a random ice plane. In the docking exercises, the shortest distances between ice O atoms and surface atoms of the AFP were ~2–4 Å, a distance appropriate for common interactions such as hydrogen bonds and van der Waals forces. To ensure that the AFP was in full contact with the chosen ice plane, no part of the AFP was positioned outside the ice plane boundaries. Thus the centering residue of a given surface patch was roughly aligned with the center of the ice plane. The docking position of the AFP was manually adjusted to allow as many surface-exposed atoms of a given surface site as possible to be in close contact with the ice.

Optimization of AFP-ice complexes

The AFP-ice complex was first subjected to energy minimization. Conjugate gradients minimization was carried out with the AMBER forcefield (Weiner et al., 1984), using the program Discover 2.9 in the package Insight II 95.0 (Biosym/MSI Co., San Diego, CA). Hydrogen atoms were added to the protein. During energy minimization, all atoms were allowed to move, except for the water O atoms of the ice slab, the positions of which were fixed. The entire AFP, including all individual atoms, was permitted to rotate and translate with respect to the ice plane. The cutoff distance was set at 12 Å for pair list generation, and the actual interatomic nonbonding potential energy functions were gradually decreased to zero over the interval 9.5–11.0 Å. RMS derivation criteria were chosen to be 0.0001 kcal/mol to obtain a minimum potential surface.

After energy minimization, the AFP-ice complex was subjected to molecular dynamics simulations. The time step used was 1 fs, and the time-dependent trajectory file was updated every 300 steps. All simulations were performed with Berendsen's algorithm at a temperature of 273 K (Berendsen et al., 1984), with a temperature coupling constant of $\tau_T = 0.1$ ps. The complex system was equilibrated for 30 ps, and the next 90 ps of trajectory was saved for data analysis. In this simulation, thermodynamic properties such as temperature, potential energy, and total energy in the trajectory were collected after the systems were fully equilibrated. The standard derivations of the total energy, potential energy, and kinetic energy and the temperature of these simulations were ~13.0, ~23.0, and ~20.0 kcal/mol and 3.6 K, respectively. Thus the simulations by molecular dynamics were judged to be fully equilibrated. It is important to note that, as in energy minimization, no constraints were imposed on the complex system during molecular dynamics simulation, other than holding the ice O atom positions fixed. Because of the large number of calculations involving two ice targets and 11 surface patches (total 22 systems), in this first round of calculation we carried out the simulations in vacuum, and the complex was not solvated, to save CPU time. After molecular dynamics simulation, an additional round of energy minimization was performed.

The optimization procedure, including molecular docking, energy minimization, molecular dynamic simulation, and an additional round of energy minimization, was carried out for all 11 surface patches against the two ice planes. The interaction or binding energy was calculated using the following expression:

$$\Delta E_{\text{interaction}} = E_{\text{complex}} - (E_{\text{AFP}} + E_{\text{ice}})$$

Further optimization of solvated AFP-ice complexes

In the second round, the top four systems in both ice series that had the most favorable interaction energy with the ice lattices were solvated for further optimization. The starting systems were those that had already been optimized from the in vacuo calculations. To simulate the system of the AFP adsorbed on ice surrounded by aqueous solution, the AFP-ice systems were placed in $50 \times 44 \times 44$ Å^3 and $48 \times 48 \times 48$ Å^3 boxes for AFP–random ice and AFP–prism ice, respectively. In these boxes, water molecules were added using the Insight II 95.0 program (Biosym/MSI Co.). Sol-

TABLE 1 Various surface patches and residues involved

Surface patches	Centering residue	Residues in contact with ice after optimization (4 Å cutoff distance)
Patch 1	T15	L19, V20, T18, S42, V41, Q9, P12, A16, M21, T15, Q44, I13, N14, K61
Patch 2	V60	A65, A64, Y63, G62, K61, D58, R39, N46, V60, I13, R47, P57, N14
Patch 3	R23	L19, V20, N8, L51, R23, S24, E25, V26, V27, A1, A3, Q2
Patch 4	V30	E35, Q2, A65, A1, V30, A64, M56, P57, P33, R39
Patch 5	M59	T28, T53, M56, P50, P29, L10, M59, A48, D58, R47, M59, L51
Patch 6	P57	A1, V30, P29, Q2, D58, P57, E35, A64, A65, P33, M56
Patch 7	V41	G62, A64, A65, M43, R39, P38, V41, S42
Patch 8	Q44	A16, A64, V41, S42, M43, Q44, G62, K61, V49, I13
Patch 9	V49	I13, R47, A48, V49, L10, D58, M59, P50, T53, M56, P29, T28
Patch 10	E35	E35, A34, P33, A2, A1, V30
Patch 11	T53	L10, L51, P50, T53, G52, V27, T28, P29

vation was completed by placing the system in an equilibrated 3D box of solvent and removing those water molecules that overlapped with protein or ice atoms in the system being solvated. The final AFP–random ice system contained ~9554 atoms, including 2519 solvent atoms, and the final AFP–prism ice system contained ~10,652 atoms, including 2738 solvent atoms. Solvated systems were initially subjected to conjugate gradient minimization in which the protein and ice atoms were held fixed and only the solvent water molecules were allowed to move freely. Before molecular dynamics simulation, a further round of energy minimization was carried out in which only the positions of the O atoms of the ice slab were fixed. In the course of dynamic simulation, periodic boundary conditions were applied, and explicit minimum-image conventions were used in the nonbond routines. The simulation was equilibrated for 90 ps, followed by a trajectory covering 210 ps. Other details of the optimization and energy assessment were the same as those of the in vacuo calculations described above.

RESULTS AND DISCUSSION

Random ice

Unlike type I AFP, the ice lattice plane and the direction to which type III AFP binds have not been unequivocally determined. The only indication came from a study by Cheng and DeVries (1991), who reported briefly from their preliminary ice-etching studies that type III AFP might bind preferentially to the prism plane. With the uncertainty about which ice lattice plane(s) type III AFP binds, we wanted to avoid potential bias and hence employed a strategy in which both a primary prism plane and a "random" ice plane were considered. We hope that, in the absence of the knowledge of the precise ice plane(s) to which type III AFP binds, this random ice approach might provide a more unbiased evaluation of the interactions between ice and type III AFP.

When ice fronts grow, the surface layers of the ice lattice would be much less ordered than the interior lattice. A more extreme view would be that the ice surface, while it is still growing, might resemble water structure more than it does ice structure. If this is the case, we may envisage that randomly positioned water molecules in front of the ice lattice ("sluggish" surface water or "semiordered" water) are first contacted by AFPs.

AFP model from optimization

Molecular dynamics simulations can have a large impact on protein structure integrity, particularly in cases where no constraints are imposed. An appropriately restrained molecular dynamics simulation can often be employed to avoid excessive structure distortion. Because the type III AFP structure is both compact and stable (Jia et al., 1996; Sönnichsen et al., 1996), and to avoid biasing the model with unnecessary constraints, it was decided that the initial simulation could be performed without any constraints. After the initial simulation of the AFP-ice system, we compared all 22 resulting AFP structures with the original crystal structure (Jia et al., 1996). By means of least-squares fitting, we have superimposed each optimization-derived model on the x-ray structure (Fig. 1). The results are tabulated in Table 2, which shows that RMS deviations range from 1.8 to 2.7 Å. The largest differences between the x-ray structure and the resulting models were mainly localized in the N-terminal region, which is very likely to be intrinsically flexible.

Interaction between AFP and random ice

As the main purpose of this study is to investigate the binding interaction between type III AFP and ice through computational approaches that focus on energy calculations, emphasis has been placed on the evaluation of interaction energies. Interaction energies between the AFP and ice are listed in Table 3, in which patch 1 (Fig. 2) is shown to have the most favorable interaction energy. This means, from an energetic point of view, that this surface patch is more favorable for interaction with the random ice. Furthermore, there is a good energy discrimination between this patch and the next best patch. The interaction energy of patch 2 is only 86.3% of that of patch 1, corresponding to an increase of 33 kcal/mol. The interaction energies of other patches increase very quickly, approaching 19.0% of that of patch 1 for the last patch, patch 11. Using the random ice plane as an interacting target, it is evident that patch 1 is not only the best ice-binding patch, but also that there is a significant discrimination among various patches.

Interaction between AFP and prism ice

It is commonly believed that the prism ice plane is preferred by fish type III AFP, and many modeling studies have been undertaken based on this assumption (Jia et al., 1996; Sön-

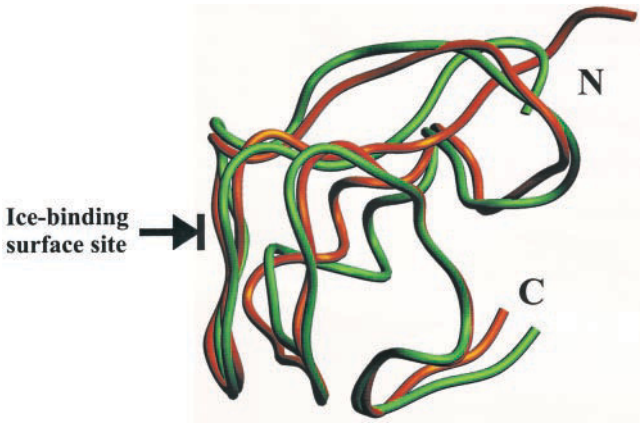

FIGURE 1 Ribbon diagram of the optimized AFP structure (*green*) derived from patch 1 of the AFP-random ice series, with the main chain overlapped by the original x-ray structure (*red*), using LSQKAB in the CCP4 suite (1994). This diagram was generated with Setor (Evans, 1993).

TABLE 2 RMS derivation (in Å) between the x-ray structure and the type III AFP models derived from the optimized AFP-ice complexes

	Random ice series			Prism ice series		
RMSD (Å)	Non-H atom	Backbone	Cα	Non-H atom	Backbone	Cα
Patch 1	2.42	2.18	2.20	2.66	2.41	2.42
Patch 2	2.28	2.02	2.07	2.34	2.07	2.10
Patch 3	2.28	2.07	2.08	2.30	2.06	2.08
Patch 4	2.43	2.22	2.25	2.48	2.26	2.29
Patch 5	2.29	2.08	2.11	2.25	2.06	2.09
Patch 6	2.32	2.10	2.14	2.31	2.05	2.09
Patch 7	2.31	2.09	2.11	2.24	2.03	2.05
Patch 8	2.31	2.10	2.22	2.23	1.99	2.01
Patch 9	2.35	2.13	2.16	2.43	2.18	2.21
Patch 10	2.35	2.13	2.16	2.37	2.12	2.16
Patch 11	2.32	2.10	2.12	2.33	2.12	2.14

nichsen et al., 1996; Yang et al., 1998; DeLuca et al., 1998; Graether et al., 1999), although it lacks explicit support from experimental evidence. To investigate this assumption, a primary prism ice plane was used as an interacting target; the results are given in Table 3. As in the case of random ice, patch 1 ranked first among all surface patches. Because the distributions of water molecules in the two ice slabs are different, it is not possible to directly compare the energy between the two series. There are nevertheless some common characteristics to be noted. In the prism ice series, once again patch 1 (Fig. 2) is not only the most favorable ice-binding patch but also has a significantly better interaction energy than the second best patch. Similar to the random ice series, interaction energy increases quickly for other patches, although the exact ordering of the patches is somewhat different between the two series.

More extensive molecular dynamics simulation of the solvated system

To further characterize and ascertain the AFP-ice interaction derived from the in vacuo calculations, simulations of the solvated system were carried out. In addition, more extensive molecular dynamics were used in this second round of calculations. Because of the large number of systems to be computed, however, only the top four systems in the two ice series were selected. Even after longer (300 ps) unrestrained dynamic simulations, the RMS deviations calculated from nonhydrogen atoms between the resulting models and the x-ray structure were all below 3.0 Å, which is only slightly higher than those of the shorter (120 ps) in vacuo calculations. As shown in Table 4, the ordering of the top four patches remains the same, and there is still appreciable energy discrimination. Using the hydrogen bond, an interaction that can be directly visualized, as an indicator, we found an excellent agreement between the two rounds of calculations. In patch 1, for example, in both simulations the side chains of the same residues of type III AFP formed hydrogen bonds with the ice lattice. These residues were Q9, N14, T15, T18, S42, Q44, and K61. Evidently, the results derived from the more extensive molecular dynamics simulations of the solvated system are in excellent agreement with the short in vacuo calculations.

TABLE 3 AFP-ice interaction energy from the in vacuo simulations

Surface patch	Interaction energy with random ice (kcal/mol)	Surface patch	Interaction energy with prism ice (kcal/mol)
Patch 1	−241.6	Patch 1	−184.8
Patch 2	−208.6	Patch 2	−159.2
Patch 3	−134.4	Patch 4	−131.6
Patch 4	−131.8	Patch 8	−99.8
Patch 5	−124.5	Patch 3	−92.5
Patch 6	−107.9	Patch 5	−80.1
Patch 7	−103.5	Patch 9	−72.0
Patch 8	−98.0	Patch 7	−63.5
Patch 9	−86.2	Patch 10	−61.6
Patch 10	−84.0	Patch 6	−50.1
Patch 11	−45.9	Patch 11	−47.0

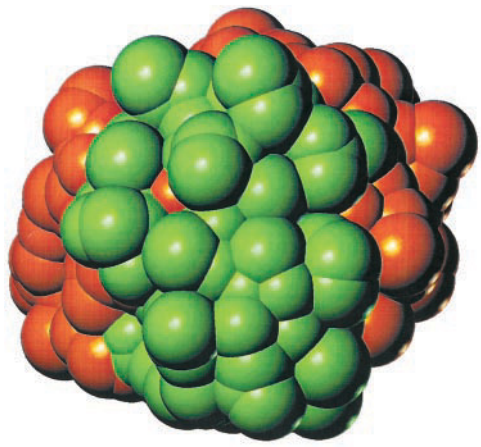

FIGURE 2 Space-filling model of type III AFP, highlighting the patch 1 surface site (*green*). The orientation reflects a rotation of ~90° from Fig. 1. This diagram was generated using Sybyl, version 6.4 (Tripos, St. Louis).

TABLE 4 AFP-ice interaction energy from the solvated simulations

Surface patch	Interaction energy with random ice (kcal/mol)	Surface patch	Interaction energy with prism ice (kcal/mol)
Patch 1	−239.8	Patch 1	−177.9
Patch 2	−204.8	Patch 2	−164.2
Patch 3	−132.9	Patch 4	−124.1
Patch 4	−123.1	Patch 8	−100.5

Comparison to experimental results

A series of site-directed mutagenesis experiments indicated a cluster of surface polar residues affecting AFP's ice-binding activity (Chao et al., 1994). These residues included N14 (N14 > S, 25% activity), T18 (T18 > A, 70% activity), Q9 (Q9 > T, 70% activity), and Q44 (Q44 > T, 50% activity). Further structural studies (Jia et al., 1996; DeLuca et al., 1998), along with more mutations (DeLuca, 1997), revealed that T15 (T15 > A, 70% activity) and A16 (A16 > H, 25% activity) in the proximity of previously identified residues (N14, T18, Q9, and Q44) were also involved in ice binding. In addition to these hydrophilic residues, other residues, including hydrophobic ones near this surface plane, were recently implicated to play some peripheral roles in AFP-ice interactions (Graether et al., 1999). Most of these residues are all clustered in one surface region that is believed to be the ice-binding site of type III AFP. Using 4 Å as the cutoff distance, our resulting models show that one or more atoms from 14 residues (L19, V20, T18, S42, V41, N9, P12, A16, M21, T15, Q44, I13, N14, and K61) are found to be potentially able to interact with ice. In comparison, using the same cutoff distance (4 Å), the previous docking model (Jia et al., 1996) indicated only V20, T18, M21, Q9, A16, T15, N14, Q44, and P12 to be in contact with ice. Hence the molecular dynamics simulation studies reported here give five more residues (L19, S42, V41, I13, and K61) in contact with ice. In addition to the activity mutants described above, V20, M21, I13, L19, and V41 have recently been implicated in ice binding as well (Graether et al., 1999). Furthermore, mutations of K61 have been known to affect ice crystal growth (Chao et al., 1994; DeLuca, 1997), but K61 was considered to be too far away from the ice lattice in the previous ice-docking model (Jia et al., 1996). This has in part led Jia et al. (1996) to propose that the AFP might simultaneously interact with the prism and basal planes of ice. In the current study this basal plane binding may not necessarily be required, because the K61 side chain appears to contact the prism ice plane directly, as evidenced in molecular dynamics simulation. This result would certainly influence our view of two-plane binding. Taken together, we suggest that the ice-binding site may be larger than previously suggested. Inclusion of peripheral hydrophobic residues surrounding the core cluster of hydrophilic ice-binding residues would enlarge the ice-binding site, which may have implications for understanding the mode of action of globular AFPs' ice binding in general.

Previously, in addition to mutagenesis experiments, modeling studies and structural analyses based on both the high-resolution x-ray and NMR structures have strongly suggested that patch 1 is the main ice-binding site (Jia et al., 1996; Sönnichsen et al., 1996; DeLuca et al., 1998). Moreover, an independent "flatness" analysis also confirmed the same ice-binding site (Yang et al., 1998). The results from the current computational investigation, which assumed no prior knowledge of mutation or flatness, unambiguously identify the same ice-binding surface. Because all surface patches of the AFP were analyzed in the same manner, the systematic computational procedure used in this study should be free of bias, which was difficult to avoid in the previous modeling and docking studies. Interestingly, the identified ice-binding surface of type III AFP seems to bind the random and prism ice planes equally well. It is possible that the preference for the prism ice plane by type III AFP is not as strong as previously thought. This would be in agreement with the fact that so far it has been very difficult to produce clear ice-etching pattern(s) for this AFP.

CONCLUSIONS

Using both random and primary prism ice planes as interacting targets, we have determined that patch 1 of fish type III AFP is the most energetically favorable ice-binding site. This finding is largely consistent with the previous site-directed mutagenesis and modeling studies, which likewise suggested that patch 1 is involved in ice binding. Our results have also shown that the ice-binding site of type III AFP appears to be larger than previously suggested. Inclusion of the peripheral hydrophobic residues supports the notion that the importance of hydrophobic residues in ice-binding is being increasingly realized. By means of molecular docking, energy minimization, and molecular dynamics simulation, this study had provided independent and unbiased evidence of a type III AFP ice-binding site.

We thank Brent Wathen for his critical reading and help with the manuscript. We are grateful to Dr. J. A. Cogardan at Universidad Nacional Autonoma de Mexico for his assistance in the use of the program package Insight II and computing facilities, and to Steffen Graether for helping with diagrams.

This work was supported by a grant from the Medical Research Council of Canada to ZJ.

REFERENCES

Berendsen, H. J. C., J. P. M. Postma, W. F. Gunsteren, A. DiNola, and J. R. Haak. 1984. Molecular dynamics with coupling to external bath. *J. Chem. Phys.* 81:3684–3690.

Collaborative Computational Project, Number 4. 1994. The CCP4 program suite for protein crystallography. *Acta Crystallogr. D.* 50:760–763.

Chao, H., F. D. Sönnichsen, C. I. DeLuca, B. D. Sykes, and P. L. Davies. 1994. Structure-function relationship in the globular type III antifreeze

protein: identification of a cluster of surface residues required for binding to ice. *Protein Sci.* 3:1760–1769.

Cheng, A., and K. M. Merz, Jr. 1997. Ice-binding mechanism of winter flounder antifreeze proteins. *Biophys. J.* 73:2851–2873.

Cheng, C. C., and A. L. DeVries. 1991. The role of antifreeze glycopeptides and peptides in the freezing avoidance of cold-water fish. *In* Life under Extreme Conditions. G. di Prisco, editor. Springer-Verlag, Berlin. 1–14.

Chou, K. 1992. Energy-optimized structure of antifreeze protein and its binding mechanism. *J. Mol. Biol.* 223:590–517.

Davies, P. L., and C. L. Hew. 1990. Biochemistry of fish antifreeze proteins. *FASEB J.* 4:2460–2468.

Davies, P. L., and B. D. Sykes. 1997. Antifreeze proteins. *Curr. Opin. Struct. Biol.* 7:828–834.

DeLuca, C. I. 1997. Ph.D. thesis. The high resolution structure of type III antifreeze protein and its implication for ice binding. Queen's University, Kingston, Ontario, Canada.

DeLuca, C. I., P. L. Davies, Q. Ye, and Z. Jia. 1998. The effects of steric mutations on the structure of type III antifreeze protein and its interaction with ice. *J. Mol. Biol.* 275:515–525.

Deng, G., D. W. Andrews, and R. A. Laursen. 1997. Amino acid sequence of a new type of antifreeze protein, from the longhorn sculpin *Myoxocephalus octodecimspinosis. FEBS Lett.* 402:17–20.

Evans, S. V. 1993. Setor: hardware lighted three dimensional solid model representations of macromolecules. *J. Mol. Graphics.* 11:134–138.

Graether, S. P., C. I. DeLuca, J. Baardsnes, G. A. Hill, P. L. Davies, and Z. Jia. 1999. Quantitative and qualitative analysis of type III antifreeze protein structure and function. *J. Biol. Chem.* 274:11842–11847.

Jia, Z., C. I. DeLuca, H. Chao, and P. L. Davies. 1996. Structural basis for the binding of a globular antifreeze protein to ice. *Nature.* 384:285–288.

Jorgensen, H., M. Mori, H. Matsui, M. Kanaoka, H. Yanagi, Y. Yabusaki, and Y. Kikuzono. 1993. Molecular dynamics simulation of winter flounder antifreeze protein variants in solution: correlation between side chain spacing and ice lattice. *Protein Eng.* 6:19–27.

Knight, C. A., C. C. Cheng, and A. L. DeVries. 1991. Adsorption of α-helical antifreeze peptides on specific ice crystal surface planes. *Biophys. J.* 59:409–418.

Lal, M., A. H. Clark, A. Lips, J. N. Ruddock, and D. N. J. White. 1993. Inhibition of ice crystal growth by preferential peptide adsorption: a molecular modelling study. *Faraday Discuss.* 95:299–306.

Madura, J. D., M. S. Taylor, A. Wierzbicki, J. P. Harrington, C. S. Sikes, and F. Sönnichsen. 1996. The dynamics and binding of a type III antifreeze protein in water and on ice. *J. Mol. Struct.* 388:65–77.

Madura, J. D., A. Wierzbicki, J. P. Harrington, R. H. Maughon, J. A. Raymond, and C. S. Sikes. 1994. Interactions of the D- and L-forms of winter flounder antifreeze peptide with the (201) planes of ice. *J. Am. Chem. Soc.* 116:417–418.

McDonald, S. M., J. W. Brady, and P. Clancy. 1993. Molecular dynamics simulations of a winter flounder "antifreeze" polypeptide in aqueous solution. *Biopolymers.* 33:1481–1503.

Nicholls, A., R. Bharadwaj, and B. Honig. 1993. Grasp: graphic representation and analysis of surface properties. *Biophys. J.* 64:116–170.

Raymond, J. A., and A. L. DeVries. 1977. Adsorption inhibition as a mechanism of freezing resistance in polar fishes. *Proc. Natl. Acad. Sci. USA.* 74:2589–2593.

Sönnichsen, F. D., C. I. DeLuca, P. L. Davies, and B. D. Sykes. 1996. Refined solution structure of type III antifreeze protein: hydrophobic groups may be involved in the energetics of the protein-ice interaction. *Structure.* 4:1325–1337.

Sönnichsen, F. D., B. D. Sykes, and P. L. Davies. 1995. Comparative modeling of the three-dimensional structure of type II antifreeze protein. *Protein Sci.* 4:460–471.

Weiner, S. J., P. A. Kollman, D. A. Case, U. C. Singh, C. Ghio, G. Alagona, J. S. Profeta, and P. Weiner. 1984. A new force field for molecular mechanical simulation of nucleic acids and proteins. *J. Am. Chem. Soc.* 106:765–784.

Wen, D., and R. A. Laursen. 1992. A model for binding of an antifreeze polypeptide to ice. *Biophys. J.* 63:1659–1662.

Wierzbicki, A., J. D. Madura, C. Salmon, and F. Sönnichsen. 1997. Modeling studies of binding of sea raven type II antifreeze protein to ice. *J. Chem. Inf. Comput. Sci.* 37:1006–1010.

Wierzbicki, A., M. S. Taylor, C. A. Knight, J. D. Madura, J. P. Harrington, and C. S. Sikes. 1996. Analysis of shorthorn sculpin antifreeze protein stereospecific binding to (2–1 0) faces of ice. *Biophys. J.* 71:8–18.

Yang, D. S., W. C. Hon, S. Bubanko, Y. Xue, J. Seetharaman, C. L. Hew, and F. Sicheri. 1998. Identification of the ice-binding surface on a type III antifreeze protein with a "flatness function" algorithm. *Biophys. J.* 74:2142–2151.